ISSN- O: 2458 - 868X, ISSN–P: 2458 – 8687
National Library of Medicine - ID: 101731606

International Journal of Medical Science and Innovative Research (IJMSIR)
IJMSIR : A Medical Publication Hub
Available Online at: www.ijmsir.com
Volume – 10, Issue – 2, April – 2025, Page No. : 97 – 107

Original Article: To Evaluate The Role of Susceptibility Weighted Imaging (SWI) in Adult Cerebral Hemorrhage and Its Comparison with Gradient Echo (GRE) Sequence

[1]Dr. Sarath A S, M.B.B.S, M.D, Department of Radiodiagnosis, Gandhi Medical College, Bhopal, Madhya Pradesh, India
[2]Dr. (Mrs) Lovely Kaushal, Department of Radiodiagnosis, Gandhi Medical College, Bhopal, Madhya Pradesh, India
[3]Dr.Swati Goyal, Department of Radiodiagnosis, Gandhi Medical College, Bhopal, Madhya Pradesh, India
[4]Dr.Shubham Agrawal, Department of Radiodiagnosis, Gandhi Medical College, Bhopal, Madhya Pradesh, India
[5]Dr. Kunika Sachdeva, Department of Radiodiagnosis, Gandhi Medical College, Bhopal, Madhya Pradesh, India
Corresponding Author: Dr. Sarath A S, M.B.B.S, M.D, Department of Radiodiagnosis, Gandhi Medical College, Bhopal, Madhya Pradesh, India

Citation this Article: Dr. Sarath A S, Dr. (Mrs) Lovely Kaushal, Dr. Swati Goyal, Dr. Shubham Agrawal, Dr. Kunika Sachdeva, "Original Article: To Evaluate The Role of Susceptibility Weighted Imaging (SWI) in Adult Cerebral Hemorrhage and Its Comparison with Gradient Echo (GRE) Sequence", IJMSIR - April – 2025, Vol – 10, Issue - 2, P. No. 97 – 107.

Type of Publication: Original Research Article

Conflicts of Interest: Nil

Abstract

Introduction: Cerebral hemorrhage poses significant challenges in therapeutic management due to its potential for severe neurological consequences. Advanced imaging techniques like Susceptibility Weighted Imaging (SWI) and Gradient Echo (GRE) sequences have become vital for accurate diagnostics. SWI has garnered interest for its sensitivity to blood products, enabling enhanced visualization of hemorrhagic lesions, especially cerebral microbleeds (CMBs). However, its utility compared to GRE in detecting hemorrhages needs further exploration.

Objective: This study evaluates the diagnostic efficacy of SWI in adult cerebral hemorrhage, comparing its performance with the widely-used GRE sequence.

Methods: Conducted as a cross-sectional study at Gandhi Medical College and Hamidia Hospital, Bhopal, India, from September 2022 to December 2023, this research included adult patients with suspected intracranial hemorrhage, stroke, or conditions like cerebral amyloid angiopathy. Data were gathered on hemorrhage detection rates, area measurements, and lesion specificity across SWI and GRE, with statistical comparisons performed on these metrics.

Results: The analysis revealed that SWI identified a significantly higher number of hemorrhages (mean: 3.30 vs. GRE: 2.74, $p < 0.001$) and a larger mean hemorrhage area (654.82 mm^2 vs. GRE: 575.03 mm^2, $p = 0.001$). SWI also demonstrated greater sensitivity in detecting CMBs and hemorrhagic lesions in complex brain regions, including the basal ganglia and brain stem. Specific hemorrhage types, such as infarcts with hemorrhagic transformation and intraparenchymal bleeds, were more accurately visualized on SWI than GRE.

Conclusion: SWI outperforms GRE in detecting cerebral hemorrhages, particularly in identifying more lesions and larger areas, making it a valuable tool in neuroimaging.

Its enhanced sensitivity suggests SWI could improve diagnostic accuracy, guiding better clinical management of cerebral hemorrhage cases.

Keywords: cerebral hemorrhage; susceptibility-weighted imaging; gradient echo; microhemorrhages; diagnostic sensitivity; neuroimaging;

Introduction

Cerebral hemorrhage, defined as bleeding within brain tissue, presents serious challenges in therapeutic management due to its potential for causing substantial neurological complications. Advanced imaging techniques have become valuable tools in the quest for accurate diagnostics and improved patient outcomes. Among these techniques, Susceptibility Weighted Imaging (SWI) has gained recognition for its capability to create high-resolution images sensitive to blood products and their paramagnetic properties. The application of SWI in the context of adult cerebral hemorrhage shows promising improvements in detecting, characterizing, and understanding hemorrhagic lesions [1].

To fully evaluate its clinical utility, SWI must be compared to established imaging methods like Gradient Echo (GRE), a widely adopted technique for cerebral hemorrhage imaging. GRE's sensitivity to blood breakdown products has made it a reliable tool for detecting and characterizing hemorrhagic lesions, earning trust among clinicians. However, SWI introduces advantages such as superior sensitivity to smaller hemorrhages, enhanced spatial resolution, and the ability to distinguish blood products based on magnetic susceptibility [2].

Susceptibility-weighted imaging (SWI) excels at detecting cerebral microbleeds (CMBs), crucial markers of cerebral small vessel disease (SVD) and conditions like cerebral amyloid angiopathy (CAA) [3]. SWI provides higher contrast-to-noise ratios and enhanced spatial resolution compared to traditional T2*-weighted GRE imaging, allowing improved detection of smaller hemorrhagic changes [4]. However, SWI's sensitivity to iron-laden structures, such as veins and arteries, can complicate the differentiation of true CMBs from other regions, leading to potential false positives [5]. While SWI and GRE show high agreement in simpler cases, their reliability in complex scenarios with extensive lesions requires further research [4-6]. Standardized studies comparing SWI and GRE, alongside clinical data integration, are essential to refine diagnostic accuracy. Combining SWI's sensitivity with GRE's selectivity could optimize the detection of CMBs, improving prognostic evaluation and patient care [7].

The study focused to assess the sensitivity and specificity of SWI in detecting intracranial haemorrhage, examine the sensitivity and specificity of GRE in the same context, and directly compare the utility of SWI and GRE sequences to determine their effectiveness in identifying intracranial haemorrhage.

Materials and Methods

The study was conducted in the Department of Radiodiagnosis at Gandhi Medical College and Hamidia Hospital, Bhopal, India, from September 2022 to December 2023. It included patients with suspected intracranial hemorrhage, polytrauma cases with hemorrhage, hemorrhagic brain lesions referred from the stroke unit, cerebral amyloid angiopathy, hypertensive hemorrhage, and those on anticoagulant therapy or with bleeding disorders. Exclusion criteria comprised patients with claustrophobia, pacemakers, MRI-incompatible metallic implants, neuro-stimulator or magnetic dental implants, and aneurysmal clips. This selection ensured the inclusion of relevant cases while excluding those with contraindications to MRI imaging.

Figure 1: T2* GRE axial planning

Figure 2: SWI axial planning

Results

The study's age distribution shows the highest representation among participants over 60 (26%), followed by the 31-40 (19%), 21-30 (18%), 41-50 (16%), and 51-60 (15%) age groups, with the youngest group (20 or younger) comprising 6%. The mean age is 47.87 years (SD = 20.53), highlighting a broad age range and a focus on older adults more prone to cerebral hemorrhage. Male participants predominate, comprising 69% of the sample, compared to 31% female representation.

Table 1: Distribution as per Causes

Causes	Frequency	Percent
Calcifications	16	16.0
Cerebral Amyloid Angiopathy	4	4.0
Diffuse Axonal Injury	12	12.0
Extradural Hemorrhage	2	2.0
Hemorrhagic Contusions	3	3.0
Infarct With Hemorrhagic Transformation	22	22.0
Intraparenchymal Bleed	20	20.0
Microhemorrhages	10	10.0
Subarachnoid Hemorrhage	8	8.0
Subdural Hemorrhage	3	3.0
Total	100	100.0

The study shows that infarct with hemorrhagic transformation is the leading cause (22%), followed by intraparenchymal bleed (20%) and calcifications (16%). Diffuse axonal injury occurs in 12% of cases, microhemorrhages in 10%, and subarachnoid hemorrhage in 8%. Less common causes include cerebral amyloid angiopathy (4%), hemorrhagic contusions (3%), subdural hemorrhage (3%), and extradural hemorrhage (2%).

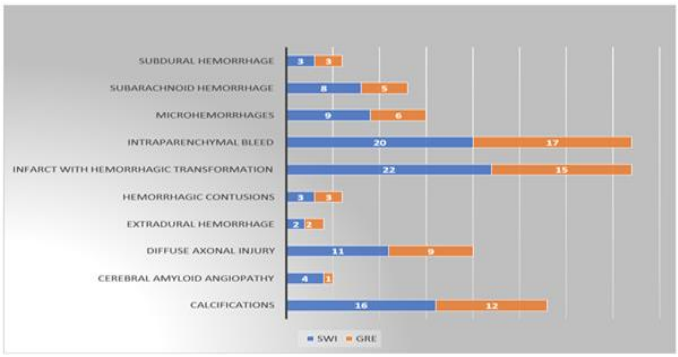

Graph 1: Comparison of Haemorrhage Presence

SWI shows higher sensitivity than GRE in detecting hemorrhages, with more cases identified in calcifications (16 vs. 12, p = 0.028), cerebral amyloid angiopathy, diffuse axonal injury, intraparenchymal bleed, microhemorrhages, and subarachnoid hemorrhage. Extradural hemorrhage, hemorrhagic contusions, and subdural hemorrhage are equally detected by both methods.

Table 2: Comparing Number of C/H between SWI and GRE

Paired Samples Statistics					
		Mean	N	Std. Deviation	P value
Pair 1	SWI Number of C/H	3.30	73	2.832	<0.001
	GRE Number of C/H	2.74	73	2.230	

SWI detects more cerebral hemorrhages on average (mean 3.30) than GRE (mean 2.74) in a sample of 73, with standard deviations of 2.832 and 2.230, respectively. The difference is statistically significant (p < 0.001), highlighting SWI's higher effectiveness in identifying cerebral hemorrhages compared to GRE.

Graph 2: Comparison of Haemorrhage Number

SWI detects more hemorrhages than GRE in most categories, with higher means for hemorrhagic contusions (4.00 vs. 3.00), infarct with hemorrhagic transformation (2.55 vs. 1.67), intraparenchymal bleeds (2.80 vs. 2.24), and microhemorrhages (3.80 vs. 3.17). While calcifications show no significant difference, SWI's enhanced sensitivity is evident overall.

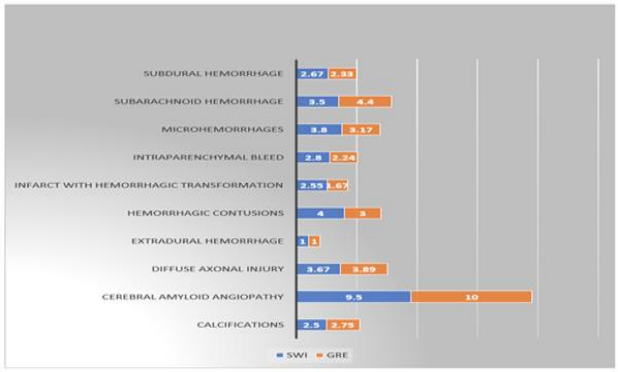

Table 3: Comparing area of C/H (in mm2) between SWI and GRE

Paired Samples Statistics					
		Mean	N	Std. Deviation	P value
Pair2	SWIAREA OF C/H (in mm2)	654.8199	73	1479.63	0.001
	GREAREA OF C/H (in mm2)	575.025	73	1394.44	

SWI detects a larger mean area of cerebral hemorrhages (654.82 mm²) compared to GRE (575.03 mm²), with both sequences having a sample size of 73. The standard deviations are 1479.63 for SWI and 1394.44 for GRE. The difference is statistically significant (p = 0.001), demonstrating SWI's superior capability.

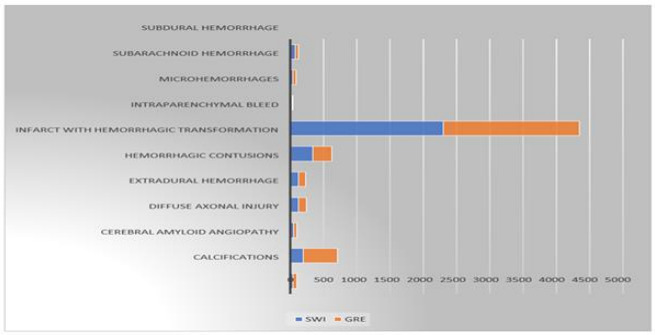

Graph 3: Comparison of Haemorrhage Area

SWI detects larger hemorrhage areas than GRE for most causes, including infarct with hemorrhagic transformation (333.30 mm² vs. 298.51 mm²), intraparenchymal bleed (2302.88 mm² vs. 2048.32 mm²), and microhemorrhages (25.90 mm² vs. 20.13 mm²). Although calcifications show a smaller mean area on SWI, the difference is not significant (p = 0.989).

Table 4: Distribution of Cerebral Hemisphere

Causes	Cerebral Hemisphere		P value
	SWI	GRE	
Calcifications	2	2	t-statistic:
Cerebral Amyloid Angiopathy	4	1	2.890
Diffuse Axonal Injury	9	7	p-value: 0.018
Extradural Hemorrhage	2	2	
Hemorrhagic Contusions	2	2	
Infarct With Hemorrhagic Transformation	19	13	
Intraparenchymal Bleed	11	10	
Microhemorrhages	10	6	
Subarachnoid Hemorrhage	8	5	
Subdural Hemorrhage	3	3	

SWI detects more hemorrhagic cases than GRE across various conditions, including cerebral amyloid angiopathy (4 vs. 1), diffuse axonal injury (9 vs. 7), infarct with hemorrhagic transformation (19 vs. 13), microhemorrhages (10 vs. 6), and subarachnoid hemorrhage (8 vs. 5). For calcifications, both detect equally, with a significant p-value of 0.018.

Table 5: Distribution of Basal Ganglia

Causes	Basal Ganglia		P value
	SWI	GRE	
Calcifications	16	12	t-statistic:1.714
Cerebral Amyloid Angiopathy	0	0	p-value:0.121
Diffuse Axonal Injury	2	2	
Extradural Hemorrhage	0	0	
Hemorrhagic Contusions	1	1	
Infarct With Hemorrhagic Transformation	0	0	
Intraparenchymal Bleed	9	6	
Microhemorrhages	1	0	
Subarachnoid Hemorrhage	0	0	
Subdural Hemorrhage	0	0	

SWI detects more basal ganglia involvement than GRE for calcifications (16 vs. 12) and intraparenchymal bleeds (9 vs. 6). Both methods detect equal cases of diffuse axonal injury (2) and hemorrhagic contusions (1), with no cases for other conditions. The p-value of 0.121 shows no significant difference for calcifications.

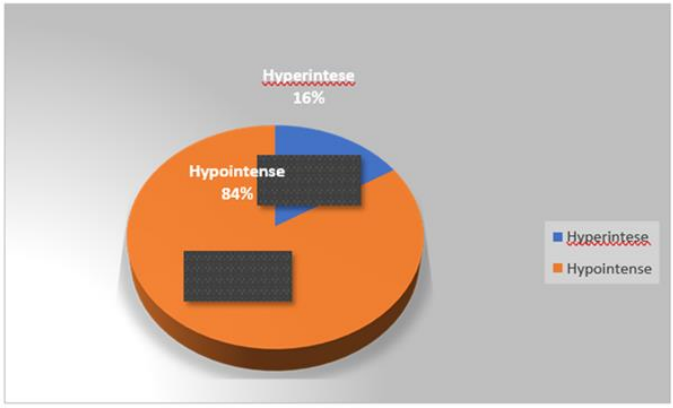

Graph 4: Distribution of patients as per phase imaging signal (SWI)

In the study population, 84% of patients exhibit hypointense signals on SWI phase imaging, while 16% show hyperintense signals, highlighting a predominant presence of hypointense signals.

Table 6: Distribution of Brain stem

Causes	Brain stem		P value
	SWI	GRE	
Calcifications	0	0	t-statistic:1.964
Cerebral Amyloid Angiopathy	0	0	p-value:0.081
Diffuse Axonal Injury	4	3	
Extradural Hemorrhage	0	0	
Hemorrhagic Contusions	0	0	
Infarct With Hemorrhagic Transformation	1	1	
Intraparenchymal Bleed	2	1	
Microhemorrhages	1	0	
Subarachnoid Hemorrhage	0	0	
Subdural Hemorrhage	0	0	

SWI detects more brain stem involvement than GRE, identifying more cases of diffuse axonal injury (4 vs. 3), intraparenchymal bleeds (2 vs. 1), and microhemorrhages (1 vs. 0). Both methods detect an equal number for infarct with hemorrhagic transformation (1), with a p-value of 0.081 indicating no significant difference.

Discussion

Our study found an average participant age of 47.87 years, with 26% over 60, emphasizing the increased vulnerability of the elderly to cerebral hemorrhage. Khaladkar SM et al. (2022) reported a similar trend, with 36% of patients over 60 years and 22% aged 50–60

years, within a total age range of 28–76 years. Research highlights age as a critical factor in brain microbleeds, as Park et al. observed an average age of 47.2 years in controls, and Sung et al. found 58 years in microbleed patients. These findings underscore age-related disorders as a major contributor to hemorrhagic events in older individuals. [8,9,10].

Our study revealed a male majority, with 69% male participants, aligning with Khaladkar SM et al. (2022), who reported 64% males and 36% females. This trend is supported by studies on imaging modalities for cerebral hemorrhages. Conklin et al. found Wave-CAIPI susceptibility-weighted imaging (Wave-SWI) more effective in males for detecting hemorrhages compared to SWI and T2*-GRE. Similarly, Juneja et al. reported a higher incidence of cerebral microbleeds in males, highlighting SWI's enhanced sensitivity, especially in hypertensive and diabetic patients. These conditions are more prevalent in males, significantly increasing their risk of cerebral hemorrhages. [8,11,12].

Punitha et al. found a higher proportion of males in their study on SWI vs. GRE for cerebral hemorrhage, supporting our findings. Firmanto et al. and Luijten et al. confirmed this trend, noting SWI's effectiveness and highlighting male prevalence, likely due to risk factors like hypertension, smoking, and alcohol use. These studies emphasize the need for targeted screening and prevention in males [13,14,15].

Our investigation found infarcts with hemorrhagic transformation (22%) and intraparenchymal bleeds (20%) as the most prevalent causes of cerebral hemorrhage, consistent with multiple studies. Wycliffe et al. found SWI more effective than other modalities in detecting bleeding with infarcts, while Akter et al. confirmed SWI's accuracy in detecting intraparenchymal bleeds. De Souza et al. and Santhosh et al. also highlighted SWI's efficacy in identifying hemorrhagic changes, supporting our findings [16,17,18,19].

Löbel et al. found SWI more efficient in detecting hemorrhages in children with diffuse intrinsic pontine glioma, aligning with our findings on intraparenchymal bleeds. Docampo et al. also supported SWI's superiority in detecting cerebral bleeding. Our study further confirms SWI's effectiveness over GRE, especially in detecting calcifications ($p = 0.028$). Cheng et al. and Sparacia et al. emphasized SWI's greater sensitivity for detecting cerebral microbleeds and cavernous malformations, supporting its use in identifying hemorrhages linked to calcifications [20,21,22,23].

Docampo et al. demonstrated that susceptibility-weighted angiography (SWAN), similar to SWI, was more sensitive than GRE in detecting cerebral hemorrhages and calcifications, supporting our findings. Santhosh et al. highlighted SWI's ability to detect early hemorrhages in infarcts. Our study found SWI detected more hemorrhages (mean 3.30 vs. GRE 2.74, $p < 0.001$), aligning with Cheng et al. (90) and Sparacia et al. (91), who also found SWI more effective in detecting cerebral microbleeds and cavernous malformations [19,21,22,23].

Our research found SWI detects larger hemorrhage areas (654.82 mm^2) compared to GRE (575.03 mm^2, $p = 0.001$), consistent with other studies. Punitha et al. observed that SWI identified larger lesions than GRE, while Löbel et al. found SWI superior in differentiating hemorrhages in pediatric diffuse intrinsic pontine glioma. Champagne et al. demonstrated that advanced SWI methods enhance hemorrhage characterization, supporting our findings of SWI's improved ability to detect and quantify larger hemorrhage areas [13,20,24].

Wang et al. found that segmented 3D echo planar acquisition SWI detected more extensive areas of bleeding than GRE in traumatic brain injury (TBI)

patients, confirming our findings of SWI's ability to identify larger hemorrhage regions. Park et al. also highlighted SWI's superiority in detecting traumatic brain microbleeds. De Souza et al. demonstrated SWI's enhanced sensitivity in detecting cerebral cavernous malformations, while Cho et al. emphasized SWI's ability to identify hemorrhagic changes within infarcts [9,18,25,26].

Conklin et al. demonstrated that Wave-CAIPI SWI surpasses conventional SWI and GRE in detecting hemorrhages and microhemorrhages, highlighting its superior diagnostic accuracy, particularly for large hemorrhagic lesions. Cho et al. confirmed SWI's enhanced sensitivity in identifying microbleeds, hemorrhages, and calcifications, supporting its advantage over GRE in the cerebral hemispheres. Similarly, Yates et al. and Miyasaka T et al. emphasized SWI's ability to detect both microbleeds and larger hemorrhagic lesions, with enhanced accuracy in delineating hemorrhage boundaries across various brain regions. These findings reinforce SWI's role as a superior neuroimaging tool for diagnosing cerebral hemorrhages and calcifications with greater precision. [11,26,27,28].

Susceptibility-weighted imaging (SWI) demonstrates higher sensitivity than gradient-recalled echo (GRE) in detecting microbleeds and intraparenchymal hemorrhages in deep brain regions like the basal ganglia and cerebellum. While no significant difference exists in calcification detection in the basal ganglia, studies by Park et al. and Miyasaka T et al. confirm SWI's superiority in identifying microbleeds across brain regions. Wycliffe et al. found SWI more effective than conventional MR and CT for hemorrhages related to acute infarcts, while Docampo et al. and Sparacia et al. highlighted its utility in detecting cavernous malformations and hemorrhagic lesions. Balzano et al. emphasized SWI's critical role in evaluating cerebral vascular abnormalities. [9,16,21,23,28,29].

Our findings confirm that susceptibility-weighted imaging (SWI) outperforms gradient-recalled echo (GRE) in detecting cerebral hemorrhages and calcifications across regions such as the cerebral hemispheres, basal ganglia, corpus callosum, and cerebellum. SWI's advanced sensitivity is particularly valuable for identifying diffuse axonal injury, intraparenchymal bleeds, and microhemorrhages, especially in challenging areas like the brainstem. Studies by Wang et al. and Cho et al. highlight SWI's superior sensitivity, while Champagne et al. and Conklin et al. validate its accuracy in detecting subtle abnormalities. Similarly, Sehgal et al. demonstrated SWI's enhanced detection of microhemorrhages and calcifications, reinforcing its critical role in neuroimaging. [11,24,25,26,30].

Conclusion

In conclusion, our study highlights the superior performance of SWI compared to GRE in detecting cerebral hemorrhages, with a particular emphasis on identifying more cases and larger hemorrhage areas across various brain regions. SWI's enhanced sensitivity allows for better visualization of diffuse axonal injuries, intraparenchymal bleeds, microhemorrhages, and calcifications, particularly in complex regions like the brain stem, basal ganglia, corpus callosum, and cerebellum. Additionally, SWI phase imaging signals, which help distinguish hemorrhagic and calcific lesions, further support its efficacy. These findings underscore the importance of integrating SWI into clinical neuroimaging to improve diagnostic accuracy and guide treatment decisions.

References

1. Hostettler IC, Seiffge DJ, Werring DJ. Intracerebral hemorrhage: an update on diagnosis and treatment.

Expert review of neurotherapeutics. 2019 Jul 3;19 (7):679-94.

2. Liu S, Buch S, Chen Y, Choi HS, Dai Y, Habib C, Hu J, Jung JY, Luo Y, Utriainen D, Wang M. Susceptibility-weighted imaging: current status and future directions. NMR in Biomedicine. 2017 Apr; 30(4):e3552.
3. Yakushiji Y. Cerebral microbleeds: detection, associations and clinical implications. New Insights in Intracerebral Hemorrhage. 2016; 37:78-92.
4. Yang J, Yang Z, Wu H, Chen W. Quantification of Iron Deposition in the Brain of Hypertensive Patients using 3D-enhanced Susceptibility-weighted Angiography (ESWAN). Current Medical Imaging. 2024 Jan;20(1):E270623218305.
5. Di Ieva A, Lam T, Alcaide-Leon P, Bharatha A, Montanera W, Cusimano MD. Magnetic resonance susceptibility weighted imaging in neurosurgery: current applications and future perspectives. Journal of neurosurgery. 2015 Dec 1;123(6):1463-75.
6. Bian W, Hess CP, Chang SM, Nelson SJ, Lupo JM. Computer-aided detection of radiation-induced cerebral microbleeds on susceptibility-weighted MR images. NeuroImage: clinical. 2013 Jan 1;2:282-90.
7. Saceleanu VM, Toader C, Ples H, Covache-Busuioc RA, Costin HP, Bratu BG, Dumitrascu DI, Bordeianu A, Corlatescu AD, Ciurea AV. Integrative approaches in acute ischemic stroke: from symptom recognition to future innovations. Biomedicines. 2023 Sep 23;11(10):2617.
8. Khaladkar SM, Chanabasanavar V, Dhirawani S, Thakker V, Dilip D, Parripati VK. Susceptibility weighted imaging: an effective auxiliary sequence that enhances insight into the imaging of stroke. Cureus. 2022 May;14(5).
9. Park JH, Park SW, Kang SH, Nam TK, Min BK, Hwang SN. Detection of traumatic cerebral microbleeds by susceptibility-weighted image of MRI. Journal of Korean Neurosurgical Society. 2009 Oct;46(4):365.
10. Sung CK, Byun JS, Yu H, Na HI, Seo JS, Kim GH. Detecting Cerebral Microbleeds on Susceptibility-Weighted MR imaging: comparison with the conventional MR imaging sequences. Journal of the Korean Society of Radiology. 2009 Feb 1;60(2):71-7.
11. Conklin J, Longo MG, Cauley SF, Setsompop K, González RG, Schaefer PW, Kirsch JE, Rapalino O, Huang SY. Validation of highly-accelerated Wave-CAIPI susceptibility-weighted imaging (SWI) compared to conventional SWI and T2*-weighted gradient-echo for routine clinical brain MRI at 3T. AJNR. American journal of neuroradiology. 2019 Dec;40(12):2073.
12. Juneja AB, Azad RA, Malhotra AN. Magnetic Resonance Imaging Evaluation of Cerebral Microbleeds: A Comparative Analysis of Susceptibility Weighted Imaging and T2* Gradient Recalled Echo Sequences. J. Clin. Diagn. Res. 2020 Sep 1;14.
13. Punitha P, Rajamanickam K, Krishnamoorthy A, Einstein A. Imaging Cerebral Haemorrhage using MRI: Improved Sensitivity of Susceptibility Weighted Imaging (SWI) Compared to Gradient Echo Sequences (GRE). Archives of Internal Medicine Research. 2020;3(1):18-25.
14. Firmanto NA, Cahyaningrum DA, Permatasari PA, Suhariningsih S, Astuti SD. Evaluation of the use of sequence T1, T2, and Susceptibility Weighted Imaging (SWI) in cases of chronic brain hemorrhage. InAIP Conference Proceedings 2023 May 19 (Vol. 2536, No. 1). AIP Publishing.

15. Luijten SP, van der Ende NA, Cornelissen SA, Kluijtmans L, van Hattem A, Lycklama a Nijeholt G, Postma AA, Bokkers RP, Thomassen L, Waje-Andreassen U, Logallo N. Comparison of diffusion weighted imaging b0 with T2*-weighted gradient echo or susceptibility weighted imaging for intracranial hemorrhage detection after reperfusion therapy for ischemic stroke. Neuroradiology. 2023 Nov;65(11):1649-55.
16. Wycliffe ND, Choe J, Holshouser B, Oyoyo UE, Haacke EM, Kido DK. Reliability in detection of hemorrhage in acute stroke by a new three-dimensional gradient recalled echo susceptibility-weighted imaging technique compared to computed tomography: a retrospective study. Journal of Magnetic Resonance Imaging: An Official Journal of the International Society for Magnetic Resonance in Medicine. 2004 Sep;20(3):372-7.
17. Akter M, Hirai T, Hiai Y, Kitajima M, Komi M, Murakami R, Fukuoka H, Sasao A, Toya R, Haacke EM, Takahashi M. Detection of hemorrhagic hypointense foci in the brain on susceptibility-weighted imaging: clinical and phantom studies. Academic radiology. 2007 Sep 1;14(9):1011-9.
18. De Souza JM, Domingues RC, Cruz LC, Domingues FS, Iasbeck T, Gasparetto E. Susceptibility-weighted imaging for the evaluation of patients with familial cerebral cavernous malformations: a comparison with T2-weighted fast spin-echo and gradient-echo sequences. American journal of neuroradiology. 2008 Jan 1;29(1):154-8.
19. Santhosh K, Kesavadas C, Thomas B, Gupta AK, Thamburaj K, Kapilamoorthy TR. Susceptibility weighted imaging: a new tool in magnetic resonance imaging of stroke. Clinical radiology. 2009 Jan 1; 64(1):74-83.
20. Löbel U, Sedlacik J, Sabin ND, Kocak M, Broniscer A, Hillenbrand CM, Patay Z. Three-dimensional susceptibility-weighted imaging and two-dimensional T2*-weighted gradient-echo imaging of intratumoral hemorrhages in pediatric diffuse intrinsic pontine glioma. Neuroradiology. 2010 Dec; 52:1167-77.
21. Docampo J, Gonzalez N, Bravo F, Sarroca D, Morales C, Bruno C. Susceptibility-weighted angiography of intracranial blood products and calcifications compared to gradient echo sequence. The neuroradiology journals. 2013 Oct;26(5):493-500.
22. Cheng AL, Batool S, McCreary CR, Lauzon ML, Frayne R, Goyal M, Smith EE. Susceptibility-weighted imaging is more reliable than T2*-weighted gradient-recalled echo MRI for detecting microbleeds. Stroke. 2013 Oct;44(10):2782-6.
23. Sparacia G, Speciale C, Banco A, Bencivinni F, Midiri M. Accuracy of SWI sequences compared to T2*-weighted gradient echo sequences in the detection of cerebral cavernous malformations in the familial form. The Neuroradiology Journal. 2016 Oct;29(5):326-35.
24. Champagne AA, Wen Y, Selim M, Filippidis A, Thomas AJ, Spincemaille P, Wang Y, Soman S. Quantitative susceptibility mapping for staging acute cerebral hemorrhages: comparing the conventional and multiecho complex total field inversion magnetic resonance imaging MR methods. Journal of Magnetic Resonance Imaging. 2021 Dec;54(6):1843-54.
25. Wang WT, Li N, Papageorgiou I, Chan L, Pham DL, Butman JA. Segmented 3D Echo Planar Acquisition for Rapid Susceptibility-Weighted Imaging: Application to Microhemorrhage Detection in

Traumatic Brain Injury. Journal of Magnetic Resonance Imaging. 2022 Nov;56(5):1529-35.

26. Cho KH, Kim JS, Kwon SU, Cho AH, Kang DW. Significance of susceptibility vessel sign on T2*-weighted gradient echo imaging for identification of stroke subtypes. Stroke. 2005 Nov 1;36(11):2379-83.
27. Yates PA, Villemagne VL, Ellis KA, Desmond PM, Masters CL, Rowe CC. Cerebral microbleeds: a review of clinical, genetic, and neuroimaging associations. Frontiers in neurology. 2014 Jan 6; 4:205.
28. Miyasaka T, Taoka T, Nakagawa H, Wada T, Takayama K, Myochin K, Sakamoto M, Ochi T, Akashi T, Kichikawa K. Application of susceptibility weighted imaging (SWI) for evaluation of draining veins of arteriovenous malformation: utility of magnitude images. Neuroradiology. 2012 Nov; 54:1221-7.
29. Balzano RF, Mannatrizio D, Castorani G, Perri M, Pennelli AM, Izzo R, Popolizio T, Guglielmi G. Imaging of Cerebral Microbleeds: Primary Patterns and Differential Diagnosis. Current Radiology Reports. 2021 Dec; 9:1-5.
30. Sehgal V, Delproposto Z, Haacke EM, Tong KA, Wycliffe N, Kido DK, Xu Y, Neelavalli J, Haddar D, Reichenbach JR. Clinical applications of neuroimaging with susceptibility-weighted imaging. Journal of Magnetic Resonance Imaging: An Official Journal of the International Society for Magnetic Resonance in Medicine. 2005 Oct;22(4):439-50.